LCA16 Disease Mutation Shows that Inner Pore Size is Critical for Kir7.1 Channel Function

Katie Beverley, Pawan Shahi, and Bikash Pattnaik
University of Wisconsin – Madison
School of Medicine and Public Health, Department of Pediatrics

UW Health American Family Children's Hospital

Department of Pediatrics
UNIVERSITY OF WISCONSIN
SCHOOL OF MEDICINE AND PUBLIC HEALTH

BACKGROUND

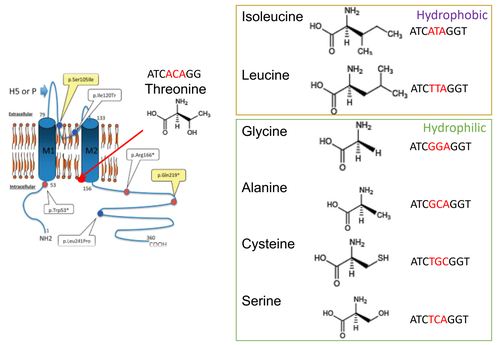

METHODS

- Molecular modeling was performed using Protean3D to determine the inner pore size of T153I, T153G, T153A, T153L, T153C, or T153S.
- Whole-cell patch-clamp electrophysiology with either extracellular Ringer's or Rb+ was performed on cell's expressing GFP tagged wildtype (WT) Kir7.1 or T153 mutants to determine channel function.
- Extracellular K+-gradient was used to determine chord conductance.
- Data analyzed using the Clampfit and ANOVA.

Mutant	Forward Primer	Reverse Primer
T153I	5'GGC CTC ATG CTA GAG GCT TTT ATC ATA GGT GCT TTT GTG3'	5'CAC AAA AGC ACC TAT GAT AAA AGC CTC TAG CAT GAG GCC3'
T153L	5'GGC CTC ATG CTA GAG GCT TTT ATC TTA GGT GCT TTT GTG3'	5'CAC AAA AGC ACC TAA GAT AAA AGC CTC TAG CAT GAG GCC3'
T153C	5'AAT CTT CGC CAC AAA AGC ACC GCA GAT AAA AGC CTC TAG CAT GAG G3'	5'CCT CAT GCT AGA GGC TAT CTG CGG TGC TTT TGT GGC GAA GAT T3'
T153A	5'CTT CGC CAC AAA AGC ACC TGC GAT AAA AGC CTC TAG CAT GAG3'	5'CTC ATG CTA GAG GCT TTT ATC GCA GGT GCT TTT GTG GCG AAG3'
T153G	5'CTT CGC CAC AAA AGC ACC TCC GAT AAA AGC CTC TAG CAT GAG3'	5'CTC ATG CTA GAG GCT TTT ATC GGA GGT GCT TTT GTG GCG AAG3'
T153S	5'GCC ACA AAA GCA CCT GAG ATA AAA GCC TCT AGC AT3'	5'ATG CTA GAG GCT TTT ATC TCA GGT GCT TTT GTG GC3'

The *inner pore size* and *polarity* are critical regulators of Kir7.1 ion conductance independent of the extracellular domain.

RESULTS

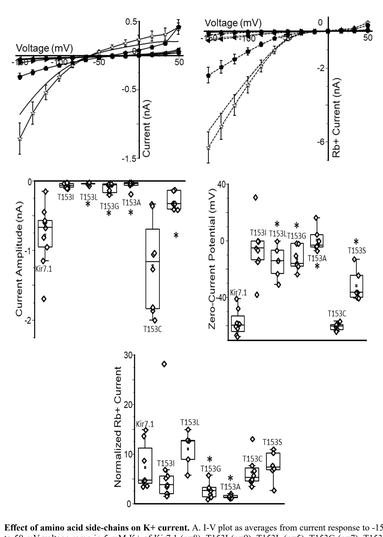

Effect of amino acid side-chains on K+ current. A. I-V plot as averages from current response to -150 to 50 mV voltage ramp in 5 mM K+ of Kir7.1 (n=8), T153I (n=9), T153L (n=5), T153G (n=7), T153A (n=7), T153C (n=8), and T153S (n=7). Symbols remain the same for panels A-B. B. Average I-V plot from current response to voltage ramp in 135 mM Rb+ for the same cells as in panel A. C. Inward-Current amplitude measured at -150 mV for alternate side-chain mutants compared to wildtype and T153I. The * indicates P-value ≤ 0.05 compared with wildtype. D. Zero-current potential calculated from panel A of alternate side-chain mutants compared to wildtype and T153I. D. Rb+ fold change calculated relative to K+ current (panel A/panel B) when cells were exposed to 135 mM Rb+.

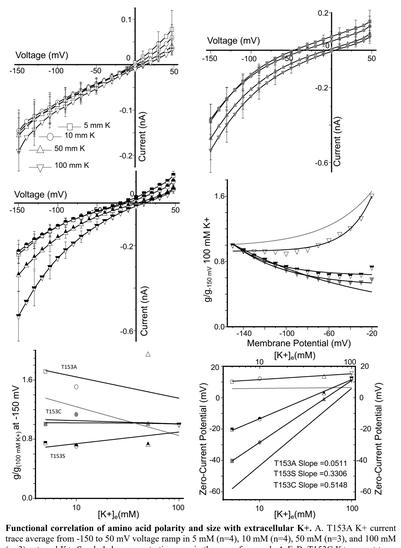

Functional correlation of amino acid polarity and size with extracellular K+. A. T153A K+ current trace average from -150 to 50 mV voltage ramp in 5 mM (n=4), 10 mM (n=4), 50 mM (n=3), and 100 mM (n=3) external K+. Symbols by concentration remain the same for panels A-F. B. T153C K+ current trace average from voltage ramp in 5 mM (n=6), 10 mM (n=6), 50 mM (n=6), and 100 mM (n=6) external K+. C. T153S K+ current trace average from voltage ramp in 5 mM (n=6), 10 mM (n=6), 50 mM (n=6) and 100 mM (n=6) external K+. D. Normalized chord conductance to 100 mM K+ (g/g_{max}) from panels A-C compared with WT and T153I across voltages (n≥3). E. Plot of g/g_{max} across external K+ concentration from panels A and B compared with WT and T153I (n≥3). F. Plot of zero current potential relative to external K+ concentration of polar and short side-chain T153 mutants compared with wildtype and T153I from panels A-C.

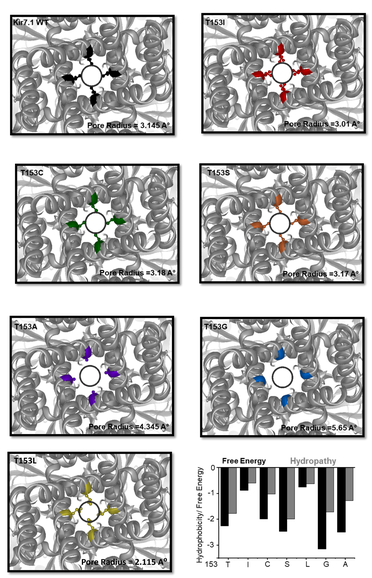

Summary

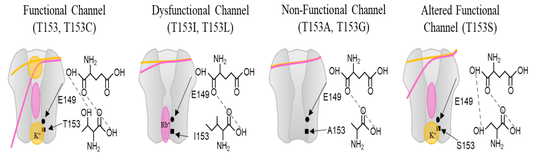

Kir7.1 structure-function correlation. Functional channels form a narrow inner pore with two hydrogen bonds (dashed lines) between the amino acid at positions 153 and 149, conducting both K+ and Rb+. Dysfunctional channels form a constricted inner pore with one hydrogen bond between amino acids at positions 153 and 149, which selectively restricts K+ conductance. Non-functional channels form a wide inner pore with one hydrogen bond between amino acids at 153 and 149. Channels with altered functions have limited K+ and Rb+ conductance.

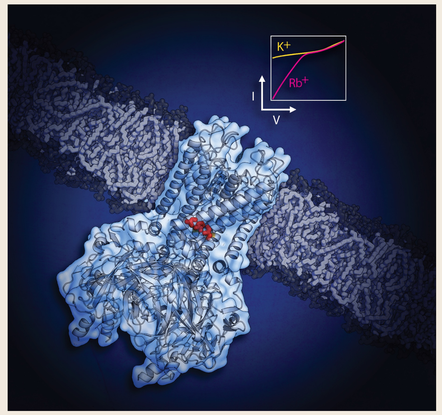

Acknowledgements

We acknowledge all past and present members of the Pattnaik lab for their insights and support of the work presented in this manuscript.

Funding: NEI, Atres Avegil,
ERP T32, Ophthalmology core

NIH National Eye Institute